

Critical velocity of a mobile impurity in one-dimensional quantum liquids

M. Schecter,¹ A. Kamenev,^{1,2} D.M. Gangardt,³ and A. Lamacraft⁴

¹School of Physics and Astronomy, University of Minnesota, Minneapolis, MN 55455, USA

²William I. Fine Theoretical Physics Institute, University of Minnesota, Minneapolis, MN 55455, USA

³School of Physics and Astronomy, University of Birmingham, Edgbaston, Birmingham, B15 2TT, UK

⁴Department of Physics, University of Virginia, Charlottesville, Virginia, 22904-4714, USA

(Dated: March 30, 2012)

We study the notion of superfluid critical velocity in one spatial dimension. It is shown that for heavy impurities with mass M exceeding a critical mass M_c , the dispersion develops periodic metastable branches resulting in dramatic changes of dynamics in the presence of an external driving force. In contrast to smooth Bloch Oscillations for $M < M_c$, a heavy impurity climbs metastable branches until it reaches a branch termination point or undergoes a random tunneling event, both leading to an abrupt change in velocity and an energy loss. This is predicted to lead to a non-analytic dependence of the impurity drift velocity on small forces.

The study of the effect of impurities constitutes a major theme in condensed matter physics. In the solid state impurities are typically regarded as *immobile*, acting as static perturbations. Prime examples include the residual resistance of metals and the Kondo effect. In other (typically liquid) states *mobile* impurities play a vital role, with the influence of ^3He impurities on the transport properties of superfluid ^4He being perhaps the best studied example [1, 2].

The traditional goal has been to understand the effect of foreign particles or defects on an otherwise pure system. However, the converse problem – to determine the effect of the surrounding medium on the motion of impurities – is increasingly relevant to the study of ultracold atomic gases. There are several ways in which mobile impurities appear naturally in these systems: (i) a small fraction of atoms may be transferred to a different hyperfine state, creating a dilute gas of distinguishable impurities of the same mass [3–5]; (ii) mixtures of different atomic species (*e.g.*, ^{87}Rb and ^{41}K in Ref. [6]) with one dilute component give a route to impurities of mass M different from the mass m of the host particles; (iii) *Ions* of Yb^+ , Ba^+ or Rb^+ have been placed in a Bose-Einstein condensate of neutral ^{87}Rb atoms [7, 8]. In each of these situations, impurity dynamics may be investigated with the help of external forces that act selectively on the impurity.

Owing to recent advances in cold atom trapping, systems in reduced dimensionalities are now well within experimental reach [5, 7, 8], bringing to light a wide range of rich and peculiar phenomena. In one spatial dimension (1D) Refs. [9, 10] established that even in the limit of strong interactions, there exists a timescale beyond which an impurity with quadratic dispersion, $E(P) = P^2/2M^*$, may propagate in a quantum fluid. In this Letter we focus on the full dispersion $E(P)$ of the resulting motion, which possesses several remarkable features not present in higher dimensions. The most prominent property is its *periodicity*, which is not evident from a quadratic, small P expansion, and may be explained as follows. The motion of N particles on a ring with circumference L results in the *total* momentum being quantized in units of

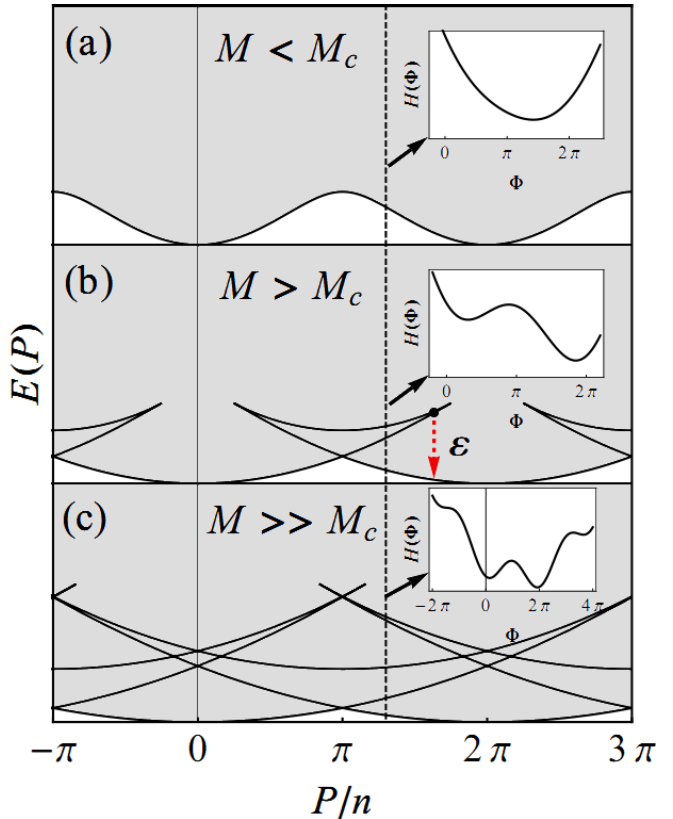


FIG. 1. Dispersion law for an impurity in a 1D quantum fluid for various impurity masses. (a) $M < M_c$, $E(P)$ is a smooth function of P and H (inset, Eq. (2)) has a single minimum. (b) $M \gtrsim M_c$, there exists a metastable minimum. An impurity driven by a force climbs a metastable branch until tunneling or H loses its minimum. Each cycle releases energy ε to the system. (c) $M \gg M_c$, many minima co-exist.

$2\pi\hbar N/L = 2\pi\hbar n$, where n is the one-dimensional density of the fluid. On the other hand, in the thermodynamic limit $N, L \rightarrow \infty$, $N/L = n$, this motion costs no kinetic energy due to infinite total mass Nm . Thus, instead of paying macroscopic energy $(2\pi\hbar n)^2/2M^*$ to

deliver this momentum to impurity motion, the system channels it to the superflow of the background liquid at no energy cost. As a result, the dispersion of the dressed impurity is a periodic function $E(P) = E(P + 2\pi\hbar n)$. Owing to the quadratic dispersion near $P = 0$, impurity motion costs less energy for a given momentum than the softest excitations of the liquid, *i.e.*, phonons with linear dispersion. This fact implies that impurity motion, while possessing a periodic dispersion, also defines the lower edge of the many-body continuum, above which (shaded grey, Fig. 1) there exist excitations comprised of the moving impurity and phonons [11–14]. Explicit examples demonstrating these features are furnished by models solvable via Bethe Ansatz [15–17]. A dramatic consequence of the dispersion periodicity is the possibility of observing Bloch oscillations of a driven impurity in 1D *in the absence of a lattice* [18, 19].

The same picture of momentum transferred to the fluid at no energy cost leads to the prediction of vanishing Landau critical velocity in 1D [20, 21]. It was shown that an *infinitely massive* object moving with any nonzero velocity with respect to the background nucleates phase slips corresponding to one quantum $2\pi\hbar n$ of total momentum transferred to the fluid. The finite rate of this process can then be related to the energy and momentum dissipation in the liquid, precluding superfluidity. On the other hand, a mobile impurity with *finite mass* M can propagate without dissipation at zero temperature with velocity given by slope of the dispersion $V = \partial E / \partial P$. Hence, the maximum slope of the dispersion defines a non-zero critical velocity for light mobile impurities.

The main result of this work is the prediction that the above regimes of heavy and light impurities are separated by a quantum phase transition taking place at a critical mass M_c , given by Eq. (3). We show that above the critical mass the many-body ground state in a total momentum sector P has cusps at $P = \pm\hbar\pi n, \pm 3\hbar\pi n, \dots$, while the impurity dispersion develops a swallowtail structure with metastable branches shown in Fig. 1. In this case the true *thermodynamic* critical velocity \mathcal{V}_c , given by the maximal slope of the many-body ground state, should be distinguished from the *dynamic* critical velocity V_c obtained from the maximal slope of the metastable branch. It can be shown that for $M \gg M_c$ the thermodynamic critical velocity is inversely proportional to M consistent with the infinite mass limit of Refs. [20, 21].

Metastability and two definitions of critical velocity. For a concrete example of how a metastable impurity dispersion can arise, let us take our fluid to be a weakly interacting Bose gas. At the mean field level, appropriate for weak interactions, the condensate wavefunction develops a phase drop Φ across the impurity located at X . In the limit of strong coupling between gas and impurity, the latter gives rise to the Josephson term

$$H_d(\Phi) = -nV_c \cos \Phi \quad (1)$$

(we have set $\hbar = 1$) in the impurity energy. Here V_c is the dynamical critical velocity which depends on the

details of the impurity. The phase drop inevitably creates a background supercurrent contributing a term $n\Phi$ to the *total* momentum P . The total energy of the impurity and the background can then be written as

$$H(P, \Phi) = \frac{1}{2\mathcal{M}}(P - n\Phi)^2 + H_d(\Phi) \quad (2)$$

The first term is the kinetic energy of the impurity moving with velocity $V = (P - n\Phi)/\mathcal{M}$, where \mathcal{M} is the total mass of the impurity and induced depletion cloud. As we shall see one can assume $\mathcal{M} \simeq M$ for a sufficiently heavy impurity.

The phase drop Φ represents a collective coordinate characterizing the state of the impurity equilibrated with the background [19]. Its value is determined from the requirement of the minimum of the total energy (2) leading to the matching $P - n\Phi = MV_c \sin \Phi$ of the Josephson current $nV_c \sin \Phi$ to the current nV experienced by the impurity in its rest frame. For sufficiently large mass $M > M_c$ this equation has several solutions corresponding to different arrangements of the impurity and the background. The total energy $H(P, \Phi)$ in Eq. (2) can therefore have minima for several values of the phase drop Φ for a given value of the total momentum P . Plotting the corresponding energies results in a typical swallowtail structure for the dispersion, see Fig. 1.

Following the global minimum $E_-(P)$ of the dispersion one sees that it develops cusps at the crossing points $P = \pm\pi n, \pm 3\pi n, \dots$ corresponding to a first order transition as a function of the total momentum P . In addition to the true ground state $E_-(P)$ there is also a metastable branch $E_+(P)$ corresponding to local minimum. The minima corresponding to $E_-(P)$ and $E_+(P)$ are separated by the maximum. At the termination points P_t the maximum merges with the local minimum at $\Phi = \Phi_t$ and the metastable branch ceases to exist. The critical mass M_c for the swallowtail catastrophe can be estimated from the simple model Eq. (2) as

$$M_c = \pi n / V_c = Km(c/V_c), \quad (3)$$

where $K = \pi n/mc$ is the Luttinger parameter of the liquid depending on the speed of sound c . For a strongly repulsive impurity in a weakly interacting background $M_c \gg m$ since $K \gg 1$ and $c \gg V_c$, justifying *a posteriori* the assumption $\mathcal{M} \simeq M$.

For $M \gg M_c$ the termination point corresponds to $\sin \Phi_t = \pm 1$ and the mass-independent velocity $\partial E_+ / \partial P = \pm V_c$. In contrast, the thermodynamic critical velocity, defined with the help of the stable branch $\mathcal{V}_c = \partial E_- / \partial P$, behaves as $1/M$ resulting in zero critical velocity for infinitely heavy impurity [20, 21].

Quantum fluctuations can smear the transition by producing a mechanism for the decay of the metastable branch [14]. The metastable branch $E_+(P)$ is well defined as long as the decay rate $\Gamma(P)$ to the lower branch satisfies $\Gamma(P) \ll E_+(P) - E_-(P) \approx 2\mathcal{V}_c|P - \pi n|$. We show below that $\Gamma(P)$ vanishes as a power law near the crossing points, $\Gamma(P) \propto |P - \pi n|^\alpha$ for $P \rightarrow \pi n$ with the

exponent α given in Eq. (7). Self-consistency therefore requires $\alpha > 1$. Hence $\alpha = 1$ is the condition defining the transition between the two classes of dispersion curves, and corresponds to $M = M_c$ [14].

Before proceeding we note that the qualitative features discussed above in no way depend upon the specific model Eq. (1) and occur (for example) in the dispersion relation of a particle moving in a Bose gas described by the Gross–Pitaevskii equation, valid for arbitrary coupling between the gas and impurity [22].

Depleton model. We now introduce a framework to describe the periodic impurity dispersion, the metastable branch, and its decay in the general case. The moving depleton, *i.e.* impurity dressed by the liquid depletion, is characterized by a number of particles N expelled from its core in addition to the phase drop Φ . The existence of the two collective slow coordinates is associated with the presence of the two conservation laws: number of particles and momentum [19]. The depleton’s dynamics is then specified by the following Hamiltonian

$$H(P, \Phi, N) = \frac{1}{2\mathcal{M}}(P - n\Phi)^2 + \mu N + H_d(\Phi, N). \quad (4)$$

Here H_d is the Φ -periodic energy function of the depletion cloud, μ is the chemical potential of the liquid in the absence of the impurity and $\mathcal{M} = M - mN$. In the limit of strongly repulsive impurity the dynamics of N is frozen and $H_d(\Phi, N)$ reduces to the simple Josephson form Eq. (1). If the mass \mathcal{M} is sufficiently large, the Hamiltonian (4) (being almost a periodic energy function of Φ) possesses many metastable minima in addition to the absolute one.

We wish to determine the tunneling rate from the above mentioned metastable minima to the ground state branch at the same momentum P . Such tunneling is accompanied by a change in the phase drop $\Delta\Phi$ and number of depleted particles ΔN , despite the momentum of both states being equal [23]. Therefore one must know the Lagrangian governing the dynamics of the collective variables Φ and N . As shown in Ref. [19], this requires the introduction of, and coupling to, the phonon subsystem. The latter may be described by small deviations of the density, $\rho(x, t)$, and velocity, $u(x, t)$, fields from their unperturbed values. It is convenient to introduce the superfluid phase $\varphi(x, t)$ and the displacement field $\vartheta(x, t)$ defined by $u = \partial_x \varphi/m$ and $\rho = \partial_x \vartheta/\pi$.

The effective action governing these harmonic degrees of freedom is that of the Luttinger liquid [25, 26]

$$S_{LL} = \frac{1}{\pi} \int dt dx \left[-\partial_x \vartheta \partial_t \varphi - \frac{c}{2K} (\partial_x \vartheta)^2 - \frac{cK}{2} (\partial_x \varphi)^2 \right], \quad (5)$$

while their coupling to the depleton degrees of freedom takes a universal form [19, 24],

$$S_{int} = \int dt \left[-\dot{\Phi} \vartheta(X, t)/\pi - \dot{N} \varphi(X, t) \right]. \quad (6)$$

It is the phonon subsystem which must supply the macroscopic momentum $n\Delta\Phi$ and take away ΔN particles from

the depleton. Near the point $P = \pi n$, the phonons have only a small amount of energy ε with which to do this. This low-probability event, or ‘under-the-barrier’ evolution of the phononic system, can be described in imaginary time by performing the Wick rotation $t \rightarrow -i\tau$ in Eqs. (5), (6). We have delegated details of the tunneling calculation to a short section in the Supplemental Material [22]. We find for the tunneling rate

$$\Gamma(\varepsilon) \sim \varepsilon^\alpha; \quad \alpha = 2K \left[\left(\frac{\Delta\Phi}{2\pi} \right)^2 + \left(\frac{\Delta N}{2K} \right)^2 \right] - 1. \quad (7)$$

Writing $\varepsilon = 2V_c |P - \pi n|$ gives the momentum dependent tunneling rate advertised earlier.

The logarithmic behavior of the tunneling action [22] is valid only on the long time-scale $\tau \gtrsim l/c$, implying the validity of Eq. (7) is restricted to the regime of small ε close to $P = \pi n$. In such a case the velocities of the upper and lower branches of the dispersion are essentially opposite and close to $\pm V_c$, while the change in number of particles ΔN , being an even function of velocity, is negligible. As a result one arrives at the exponent $\alpha = 2K(\Delta\Phi/2\pi)^2 - 1$. This single collective coordinate limit, *i.e.* $\Delta N = 0$, agrees with the previous result of Ref. [28] (cf. Eq. (7.20) therein) based on a phenomenological model of tunneling between two minima in the presence of coupling to an environment. Their results also show that a finite temperature \mathcal{T} acts as a low energy cut-off, namely $\Gamma \sim \mathcal{T}^\alpha$, $\varepsilon \ll \mathcal{T}$ (see Eqs. (5.30), (7.18) of Ref. [28]).

Higher order processes involve tunneling back and forth between the two minima that become degenerate for $\varepsilon = 0$, leading to an effective spin-boson or anisotropic Kondo description [14]. The inclusion of such processes is only necessary if $\alpha < 1$, meaning that tunneling is a relevant perturbation. This leads to the rounding out of the cusp in the dispersion $E_-(P)$ at $P = \pi n$, and the disappearance of the metastable branch. Thus $\alpha = 1$ is the exact condition determining the critical mass $M = M_c$.

In the infinite mass limit with fixed velocity $V = P/M$ Eq. (4) becomes essentially a washboard potential, Fig. 1c, $H \xrightarrow[M \rightarrow \infty]{} nV\Phi + H_d(\Phi)$ (change ΔN between adjacent minima goes to zero in this limit). Thus the change $\Delta\Phi$ between the adjacent minima is exactly 2π , while the energy difference is $\varepsilon = 2\pi nV$. As a result, one finds $\alpha = 2K - 1$ and the power law dependence of the tunneling rate $\Gamma \sim V^{2K-1}$ [29] on the velocity in full agreement with the result of Ref. [20, 21].

In the limit of large energy detuning, *i.e.*, away from $P = \pi n$, the tunneling rate does not take the form (7). In this region the barrier is small and the impurity emerges from under it with only slightly less energy, despite the large detuning between the branches (see Fig. 1 insets). Therefore most of the descent from the upper branch corresponds to viscous relaxation in real time and not an under-the-barrier tunneling trajectory. Thus, near the termination momentum $P_t \simeq MV_c$, the potential may be approximated by a cubic polynomial. The dissipative

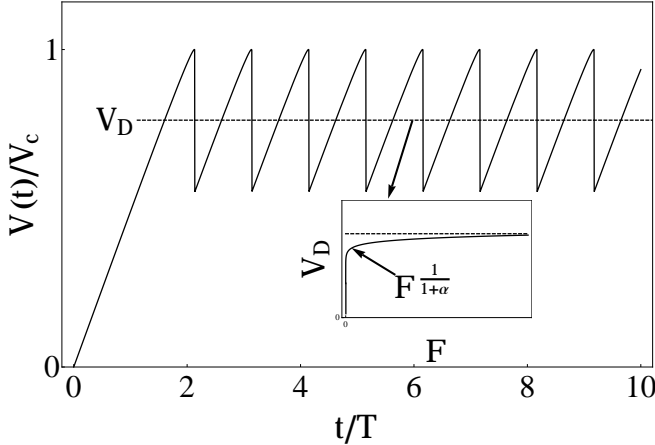


FIG. 2. Impurity velocity (solid) in units of the dynamic critical velocity V_c as a function of time in units of the period $T = 2\pi n/F$. The drift velocity is denoted by V_D (dashed) and is displayed in the inset as a function of the applied force. Due to quantum tunneling near $P = \pi n$, the drift velocity goes to zero as a power law with exponent $1/(\alpha + 1)$ (solid, inset) given by Eq. (9) for $F < F_c$ and approaches the semi-classical result for $F > F_c$ (dashed, inset) [22].

tive tunneling through such a potential was described in Ref. [30], leading to the escape rate $\Gamma \propto e^{-\bar{S}}$, where

$$\bar{S} = 2K \frac{P_t - P}{\sqrt{M^2 V_c^2 - n^2}}. \quad (8)$$

We see that for both large and small energy detuning, Eqs. (7), (8) the tunneling action scales with the Luttinger parameter K .

One way to explore the metastable branches of the dispersion is by applying an external force F to the impurity and studying the ensuing dynamics. For sufficiently strong force the driven impurity overshoots the ground state branch and follows the metastable branch until it either tunnels or reaches the termination point P_t (see Fig. 1). The energy dissipated per cycle, ε , must be supplied by external force: $FV_D = \varepsilon/T$ resulting in the drift velocity $V_D = \varepsilon/2\pi n$. Here $T = 2\pi n/F$ is the period of the motion.

Tunneling is negligible when $\Gamma T \ll 1$, which occurs if the force is sufficiently large. In such a case the external force drives the impurity all the way up to the termination point P_t . It then loses the energy minimum and relaxes to the lower branch, emitting phonons. As a result, the energy dissipated per cycle and thus drift velocity are essentially independent of the applied force. This is in stark contrast to the case of $M < M_c$, where the phonon emission due to dipole radiation gives rise to a linear in F drift velocity and hence a finite impurity mobility $\sigma = V_D/F$ [19].

The impurity velocity takes the form of a saw-tooth trajectory, experiencing a slow build-up and a sudden drop when the velocity reaches V_c , see Fig. 2. As a function of the mass, V_D saturates to the critical ve-

locity in the limit $M \rightarrow \infty$. This is most easily seen by noting that in such a limit the energy drop occurs between two adjacent and essentially parallel parabolas: $\varepsilon = 2\pi n V_D = P^2/2M - (P - 2\pi n)^2/2M \rightarrow 2\pi n V_c$. On the same grounds, the amplitude of the saw-tooth oscillations is a decreasing function of M going to zero in the infinite mass limit.

Quantum effects become dominant only if the time spent on a metastable branch is comparable with the inverse tunneling rate: $\Gamma T \gtrsim 1$. Thus, the effect of quantum tunneling plays a role only for very small forces. In this limit, the impurity is likely to tunnel at a momentum immediately above $P = \pi n$, right when it enters the metastable branch. Using the rate Eq. (7) to calculate the tunneling-averaged energy drop $\langle \varepsilon \rangle$, we find for the drift velocity [22]

$$V_D = \frac{c}{K} \left(\frac{F}{F_c} \right)^{\frac{1}{\alpha+1}}. \quad (9)$$

The non-analytic dependence of the drift on small forces is the result of the cusp of the ground state energy at $P = \pi n$ and implies the divergence of the mobility $\sigma = V_D/F$ as $F \rightarrow 0$ across the $M = M_c$ transition (see inset of Fig. 2). At finite temperature T the mobility is *not* given by $\sigma \sim T^{-\alpha}$ as might be expected due to the finite tunneling rate $\Gamma \sim T^\alpha$ near the cusp. Strictly speaking, it is given by $\sigma \sim T^{-4}$ due to two-phonon thermal Raman scattering [18, 19, 31] which results in velocity saturation *below* V_c as $F \rightarrow 0$. In practice, therefore, it is necessary to work at sufficiently low temperatures and finite drives to overcome such saturation and allow the impurity to explore the full range of momentum where metastable branches become important.

In conclusion, we have shown that the dispersion relation of a mobile impurity undergoes a sudden change when the mass of the impurity exceeds a certain critical value. The latter depends on the interaction parameter within the host liquid and thus may be varied experimentally. The predicted transition can be probed by applying an external force and monitoring either impurity velocity or excitations of the host liquid. The change of dispersion also affects the oscillation frequency and dissipation of the impurity in the trapping potential. With investigations of impurity motion in 1D atomic gases now underway [5, 7, 8], we hope that these predictions will guide future experiments.

This work was supported by the EPSRC Grant No. EP/E049095/1. MS and AK were supported by DOE contract DE-FG02-08ER46482. DMG acknowledges support by EPSRC Advanced Fellowship EP/D072514/1. AL acknowledges support of the NSF grant DMR-0846788 and the Research Corporation through a Cottrell Scholar award.

I. SUPPLEMENTAL MATERIAL

Impurity coupled to a weakly interacting liquid – To model the heavy impurity in the presence of a weakly interacting superfluid at $T = 0$, we employ the Gross-Pitaevskii equation (GPE) using a point description of the impurity wavefunction with coordinate X ,

$$i\partial_t \Psi = \left(-\frac{\partial_x^2}{2m} + g|\Psi|^2 - \mu + G\delta(x - X) \right) \Psi. \quad (10)$$

We look for a solution of the traveling wave form $\Psi(x, t) = \Psi(x - Vt)$ and $X(t) = Vt$. The usual way of dealing with a delta function perturbation is to attempt a solution constructed from two homogeneous (*i.e.*, $G = 0$) solutions that must satisfy the proper boundary conditions at $x = X$. This strategy is facilitated by the fact that the bare GPE ($G = 0$) admits a one-parameter family of solutions

$$\Psi_s(x - Vt) = \sqrt{n} \left(\frac{V}{c} - i\sqrt{1 - \frac{V^2}{c^2}} \tanh \left(\frac{x - Vt}{l} \right) \right), \quad (11)$$

known as grey solitons [32, 33]. They can be visualized as a density dip moving with velocity V , having a core size $l = \xi(1 - V^2/c^2)^{-1/2}$, where $c = \sqrt{ng/m}$ is the speed of sound, $n = \mu/g$ is the 1D density and $\xi = 1/mc$ is the healing length (the condition of weak inter-particle coupling implies $n\xi \gg 1$). Thus, by appropriately matching two solitonic solutions at $x = Vt$, one formally solves Eq. (10) with $\Psi(x - Vt)$ given by

$$\Psi(y) = \begin{cases} \Psi_s(y + x_0)e^{i\Phi_0/2}, & y > 0 \\ \Psi_s(y - x_0)e^{-i\Phi_0/2}, & y < 0 \end{cases} \quad (12)$$

where $y = x - Vt$. Here we introduced two "matching parameters" x_0 and Φ_0 which must be chosen to satisfy the two boundary conditions: $\Psi(0^+) = \Psi(0^-)$, $\Psi'|_{x=0^-}^{x=0^+} = 2mG\Psi(0)$. This results in the following two equations for Φ_0 and $z = \tanh(x_0/l)$

$$\tan \frac{\Phi_0}{2} = z \tan \frac{\Phi_s}{2}, \quad (13)$$

$$\sin^3 \frac{\Phi_s}{2} (1 - z^2) z = \frac{G}{c} \left[\cos^2 \frac{\Phi_s}{2} + z^2 \sin^2 \frac{\Phi_s}{2} \right], \quad (14)$$

where we have parameterized the velocity V by the solitonic phase Φ_s via $V/c = \cos \frac{\Phi_s}{2}$.

Equations (13), (14) permit a solution only for $V < V_c$ where $V_c = V_c(G) < c$ is the dynamic critical velocity that depends only upon the parameter G [34, 35]. This may be seen by plotting the right and left hand sides of Eq. (14). While the left hand side is bounded by a maximum, the right hand side grows quadratically with z and therefore the solution exists only for a limited range of Φ_s . For this reason we choose to parameterize the solution, Eq.(12), by the *total* phase drop across the impurity, $\Phi = \Phi_s - \Phi_0$, which permits a solution for *any* Φ .

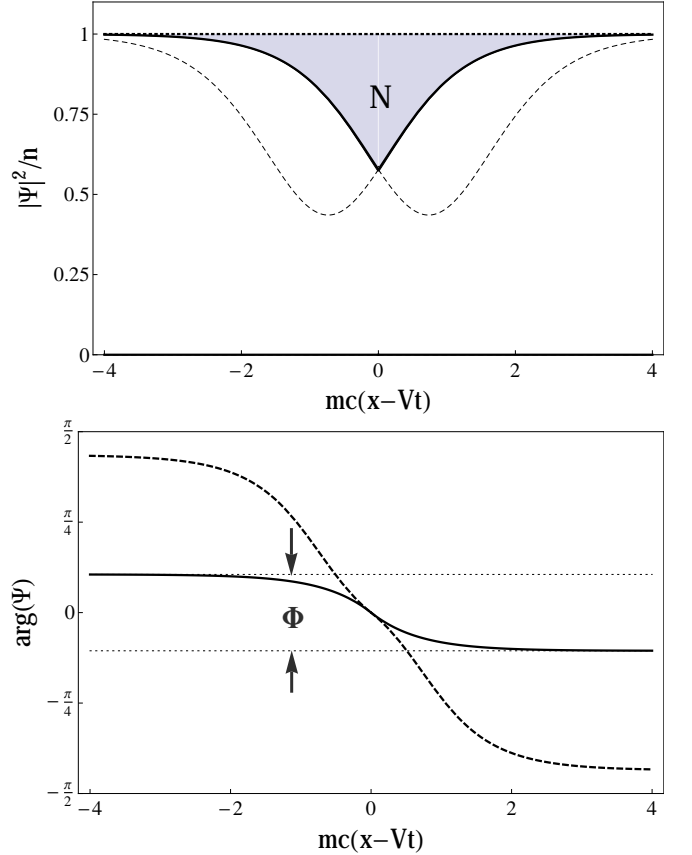


FIG. 3. Superfluid density (top panel) and phase (bottom panel) profiles in the presence of an impurity propagating with velocity $V/c = 0.66$ and coupling $G/c = 0.25$ (solid lines). The repulsive impurity tends to deplete the host liquid, pushing away N particles and inducing a phase drop Φ across it. The dashed lines correspond to the double soliton solution Eq.(11) used to construct $\Psi(x - Vt)$.

Upon solving Eqs. (13), (14) one thus finds the periodic relations $z = z(\Phi, G/c)$ and $\Phi_s = \Phi_s(\Phi, G/c)$ (*i.e.*, they are invariant with respect to $\Phi \rightarrow \Phi + 2\pi j$ for integer j).

We may use these relations to compute the dressed impurity energy $E = \frac{1}{2}MV^2 + E_d$ and momentum $P = MV + P_d$, where E_d and P_d are the corresponding depletion cloud contributions given by

$$\begin{aligned} E_d &= \int dx \left[\frac{|\partial_x \Psi|^2}{2m} + \frac{g}{2}(n - |\Psi|^2)^2 \right] + G|\Psi(X)|^2 \\ &= \frac{4}{3}nc \sin^3 \frac{\Phi_s}{2} \left[1 - \frac{3}{4}z - \frac{1}{4}z^3 \right], \end{aligned} \quad (15)$$

$$\begin{aligned} P_d &= \text{Im} \int dx [\Psi^* \partial_x \Psi] - n \arg \Psi|_{x=-\infty}^{x=\infty} \\ &= n\Phi - mNV. \end{aligned} \quad (16)$$

Here we introduced the number of expelled particles $N = \frac{2n}{mc} \sin \frac{\Phi_s}{2} (1 - z)$. Written in this way, the equilibrium expressions $E(\Phi + 2\pi j) = E(\Phi)$ and $P(\Phi + 2\pi j) = 2\pi nj + P(\Phi)$ are functions of the total phase drop Φ across the impurity, whose functional forms depend only on the

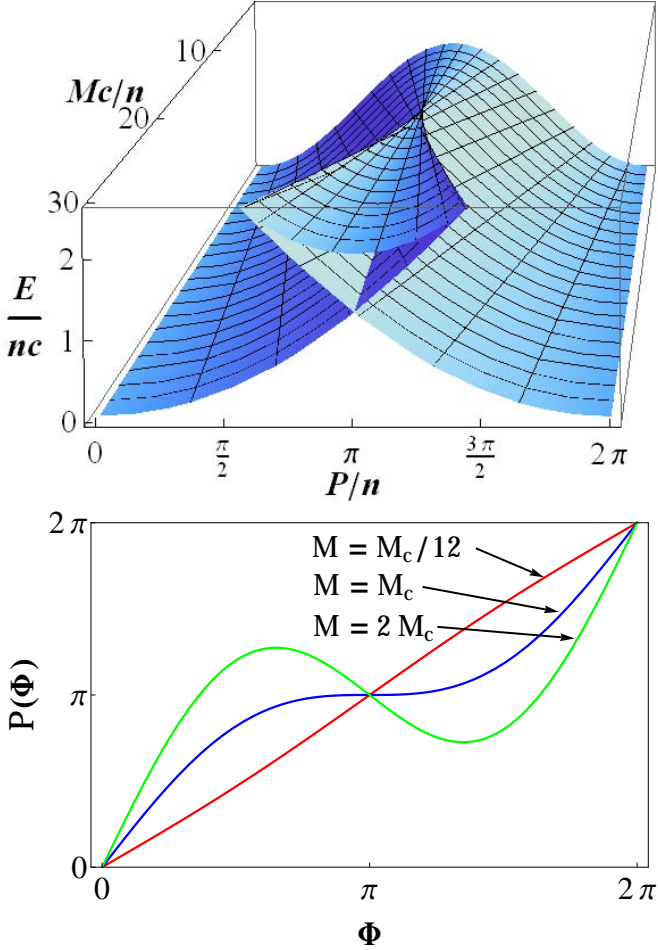


FIG. 4. Top Panel: Variation of the impurity dispersion across the $M = M_c$ transition, exhibiting the swallowtail catastrophe. Here $V_c/c = 0.1$, $K = 10\pi$ and $M_c = 12n/c$ (see Eq. (18)). Bottom panel: Momentum $P(\Phi)$ for different masses, see Eq. (17). For $M > M_c$ there persists two extrema which merge and disappear at $M = M_c$.

parameter G/c . Alternatively, one may solve for $\Phi = \Phi(P)$ with the help of Eq. (16). Substituting the resulting relation into the energy function, $E(\Phi(P))$, one obtains the periodic dispersion relation $E(P) = E(P + 2\pi n)$.

The above point description of the impurity is meaningful only if its effective mass is sufficiently large. This can be achieved either by a large bare impurity mass or strong coupling to the liquid. The latter tends to localize the impurity near the minimum of the self-induced depletion cloud density, see Fig. 3, while the former leads to a small de Broglie wavelength. To allow ourselves the generality of discussing a wide range of impurity masses, and for simplicity of illustration, we momentarily focus on the regime of strong coupling $G \gg c$.

Strong impurity coupling – We determine the dependence of z and Φ_s on Φ to leading order in c/G . From Eqs. (13), (14) we find $z(\Phi) \simeq \frac{c}{G} \cos^2 \frac{\Phi}{2}$ and $\Phi_s(\Phi) \simeq$

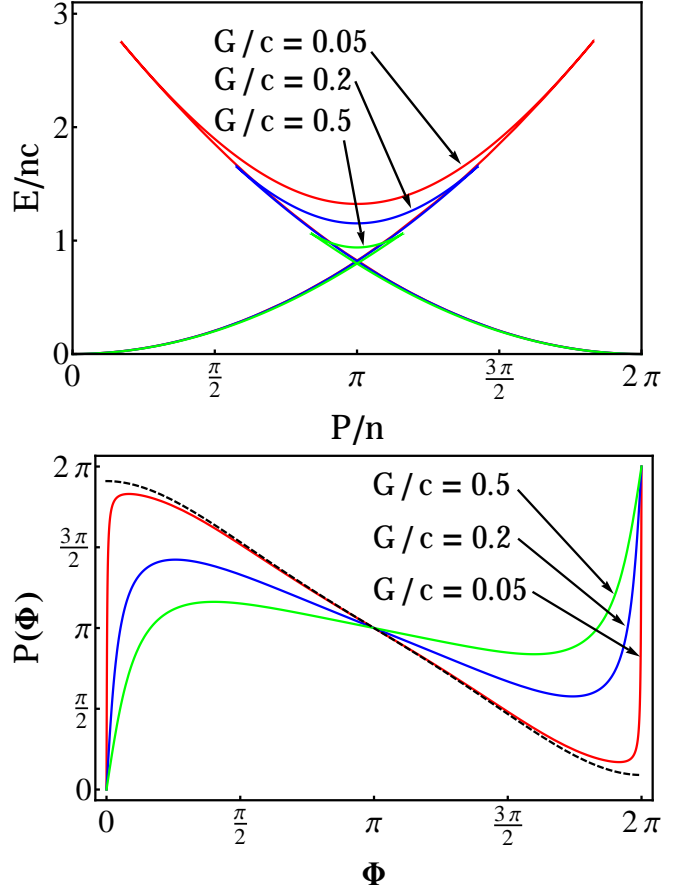


FIG. 5. Top panel: Impurity dispersion at weak coupling with parameters $M/m = 60$, $K = 10\pi$, $G/c = 0.5$ (green), $G/c = 0.2$ (blue) and $G/c = 0.05$ (red). Bottom panel: Momentum P as a function of Φ having the same parameters listed above. The $G \rightarrow 0$ limit is well approximated by the gray soliton configuration (dashed): $P = n(\Phi - \sin\Phi) + M c \cos\frac{\Phi}{2}$, except near $\Phi = 2\pi j$ for integer j , where the momentum is necessarily given by $P = 2\pi n j$.

$\pi - \frac{c}{G} \sin \Phi$ and hence,

$$P = n\Phi + \left(M - \frac{2n}{c} \right) V_c \sin \Phi. \quad (17)$$

Here the critical velocity is given by $V_c = \frac{c^2}{2G} \ll c$ [34, 35], and the Φ dependence of the velocity acquires the Josephson form: $V(\Phi) = V_c \sin \Phi$. The appearance of the critical mass occurs when $P = P(\Phi)$ is satisfied by multiple values of $\Phi(P)$. The functional form of $P(\Phi)$ for $M > M_c$ takes an "N" shape, implying the existence of two extrema in the range $\Phi \in (0, 2\pi)$, see Fig. 4. As M crosses M_c from above, these extrema merge and disappear at $P = n\Phi = \pi n$. This observation allows to derive the critical mass within the above framework,

$$\left. \frac{\partial P}{\partial \Phi} \right|_{\Phi=\pi} = 0 \implies M_c = \frac{2n}{c} \left(1 + \frac{G}{c} \right) \approx \frac{mK}{\pi} \frac{c}{V_c}, \quad (18)$$

in agreement with the parametric dependence Eq. (3) of

the main text.

Weakly coupled, heavy impurity – The case of weak impurity coupling does not lend itself to convenient analytical analysis. For given $G/c < 1$, we thus solve the boundary Eqs. (13), (14) numerically to produce the dispersion law $E(P)$, see Fig. 5. For comparison to the strong coupling case, we also plot $P(\Phi)$ for various couplings $G/c < 1$. In the limit $G \rightarrow 0$, the impurity is dressed by an essentially unperturbed gray soliton (*i.e.*, the two solitons of Fig. 3 are separated by a very small distance). This approximation breaks down near $\Phi = 2\pi j$ for integer j since we must have $P = 2\pi n j$. Consequently, there is a sharp deviation from the soliton configuration (dashed line in Fig. 5) near these points, making the functional form of $P(\Phi)$ difficult to characterize analytically. As a result of the numerical analysis, we see that even in the regime of weak coupling the appearance of multiple momenta extrema give rise to the observed swallowtail catastrophe of the energy dispersion and is thus not restricted to the Josephson limit.

Quantum tunneling and non-analytic drift – We wish to calculate the tunneling-averaged energy drop $\langle \varepsilon \rangle$ as a function of the (small) force $F = P/t$ using the momentum dependent tunneling rate $\Gamma(P)$. To this end we establish the validity of the result (7) in the main text.

The tunneling rate $\Gamma(\bar{\tau})$ is given by the exponentiated action $S(\bar{\tau})$ evaluated on the trajectory where the system tunnels for an imaginary time $\bar{\tau}$ from one minimum to the other. For $\alpha > 1$ where tunneling is an irrelevant perturbation, we may safely neglect higher order processes involving tunneling back and forth between the minima and focus on the single tunneling event. Starting from Eqs. (5), (6) of the main text (after the Wick rotation $t \rightarrow -i\tau$) one integrates the imaginary time Luttinger liquid action with linear coupling to arrive at the tunneling action

$$S(\bar{\tau}) = -\frac{1}{2} \int dx dx' d\tau d\tau' \vec{J}_{x,\tau}^\dagger(\bar{\tau}) \hat{D}(x-x', \tau-\tau') \vec{J}_{x',\tau'}(\bar{\tau}) \quad (19)$$

where $\vec{J}_{x,\tau}^\dagger(\bar{\tau}) = \delta(x-X(\tau))(\dot{\Phi}, \dot{N}) = \delta(x-X(\tau))[\delta(\tau)-\delta(\tau-\bar{\tau})](\Delta\Phi, \Delta N)$ describes the tunneling trajectory between minima having configurations which differ in phase by $\Delta\Phi$ and number of expelled particles ΔN and $\hat{D}(x, \tau)$ is the matrix imaginary time phononic propagator. The latter is determined by inverting the matrix operator of the quadratic Luttinger liquid action, Eq. (5) of the main text, in the form $S_{LL} = -\frac{1}{2} \int dx d\tau \vec{\chi}^\dagger \hat{D}^{-1} \vec{\chi}$, where $\vec{\chi}^\dagger = (\vartheta/\pi, \varphi)$.

Substituting the above tunneling trajectories into Eq. (19) with the imaginary time propagator

$$\hat{D}(x, \tau) = \frac{1}{4\pi} \begin{bmatrix} \frac{K}{\pi} \ln\left(\frac{c^2\tau^2+x^2}{l^2}\right) & \ln\left(\frac{c\tau-ix}{c\tau+ix}\right) \\ \ln\left(\frac{c\tau-ix}{c\tau+ix}\right) & \frac{\pi}{K} \ln\left(\frac{c^2\tau^2+x^2}{l^2}\right) \end{bmatrix}, \quad (20)$$

we find $S(\bar{\tau}) = (1+\alpha)\ln(c\bar{\tau}/l)$ where $l \gtrsim (mc)^{-1}$ is a short distance cut-off beyond which the point-particle description of the depletions breaks down and $\alpha = 2K \left[\left(\frac{\Delta\Phi}{2\pi}\right)^2 + \left(\frac{\Delta N}{2K}\right)^2 \right] - 1$. The X dependence of the action is neglected because it enters as $X(\tau) - X(\tau') \approx V(\tau - \tau') \ll c(\tau - \tau')$.

The energy-dependent tunneling rate is found with the help of the Fourier transformation, $\Gamma(\varepsilon) \sim \int dt e^{-S(it)} e^{i\varepsilon t}$, where the analytical continuation to real energy $i\varepsilon \rightarrow \varepsilon$ is accompanied by the Wick rotation $\tau \rightarrow it$. Substituting $S(\tau)$ given above and using the identity $\int dt e^{i\varepsilon t} (it)^{-(1+\alpha)} = \frac{2\pi\Theta(\varepsilon)}{\Gamma(1+\alpha)} \varepsilon^\alpha$, we arrive at Eq. (7) of the main text.

To compute $\langle \varepsilon \rangle$ one must know the probability to tunnel per unit time: $\dot{P}(t) = \Gamma(t) \text{Exp} \left[- \int_0^t dt' \Gamma(t') \right]$, which follows from the assumption that the process is Markovian. By parameterizing the average over time by an average over momenta one finds

$$\langle \varepsilon \rangle = \int_{n\pi}^{P_t} dP \varepsilon(P) \frac{\Gamma(P)}{F} \text{Exp} \left[- \int_{n\pi}^P dP' \frac{\Gamma(P')}{F} \right] \quad (21)$$

$$= \int_0^{F_\pi/F} dx \varepsilon(P(x)) e^{-x}. \quad (22)$$

Here we introduced the dimensionless variable $x(P) = \int_{n\pi}^P dP' \Gamma(P')/F$ along with $F_\pi = \int_{n\pi}^{P_t} dP' \Gamma(P')$. Due to the exponential decay of the kernel in Eq. (21), the integral is cut at $x_c = \min\{1, F_\pi/F\}$. As a result, one obtains the approximation $\langle \varepsilon \rangle \sim x_c \varepsilon(P_c)$, where P_c satisfies $x_c = \int_{n\pi}^{P_c} dP \Gamma(P)/F$. For $F \ll F_\pi$, we have $x_c = 1$ and hence P_c may be solved by writing $P_c = n\pi + \delta P$ for small, yet undetermined, δP . Expanding Γ near $n\pi$ as $\Gamma = \Gamma_\pi [(P - n\pi)\mathcal{V}_c/mc^2]^\alpha$, we find $\delta P = \frac{mc^2}{\mathcal{V}_c}(F/F_c)^{\frac{1}{1+\alpha}}$ and $F_c = \frac{\Gamma_\pi mc^2}{\mathcal{V}_c(1+\alpha)} \approx \frac{\Gamma_\pi M c}{2K^2}$ for large M . Thus,

$$\langle \varepsilon \rangle = mc^2 \left(\frac{F}{F_c} \right)^{\frac{1}{1+\alpha}} \implies V_D = \frac{c}{K} \left(\frac{F}{F_c} \right)^{\frac{1}{1+\alpha}}, \quad (23)$$

establishing Eq. (9) of the main text.

-
- [1] L. D. Landau and I. M. Khalatnikov, Zh. Eksp. Teor. Fiz. **19**, 637 (1949); **19**, 709 (1949).
- [2] G. Baym and C. Ebner, Phys. Rev. **164**, 235 (1967).
- [3] A. P. Chikkatur, A. Görlitz, D. M. Stamper-Kurn, S. Inouye, S. Gupta, and W. Ketterle, Phys. Rev. Lett. **85**, 483 (2000).
- [4] A. Schirotzek, C. H. Wu, A. Sommer, and M. W. Zwierlein, Phys. Rev. Lett. **102**, 230402 (2009).
- [5] S. Palzer, C. Zipkes, C. Sias, and M. Köhl, Phys. Rev. Lett. **103**, 150601 (2009).
- [6] J. Catani, L. DeSarlo, G. Barontini, F. Minardi, and M. Inguscio, Phys. Rev. A **77**, 011603 (2008).

- [7] C. Zipkes, S. Palzer, C. Sias, and M. Köhl, *Nature* **464**, 388 (2010).
- [8] S. Schmid, A. Härter, and J. H. Denschlag, *Phys. Rev. Lett.* **105**, 133202 (2010).
- [9] S. Akhanjee, Y. Tserkovnyak, *Phys. Rev. B* **76**, 140408(R) (2007).
- [10] M. B. Zvonarev, V. V. Cheianov, and T. Giamarchi, *Phys. Rev. Lett.* **99**, 240404 (2007).
- [11] M. B. Zvonarev, V. V. Cheianov, and T. Giamarchi, *Phys. Rev. B* **80**, 201102 (2009).
- [12] A. Imambekov and L. I. Glazman, *Phys. Rev. Lett.* **100**, 206805 (2008).
- [13] A. Kamenev and L. I. Glazman, *Phys. Rev. A* **80**, 011603(R) (2009).
- [14] A. Lamacraft, *Phys. Rev. B* **79**, 241105(R) (2009).
- [15] C. N. Yang and C. P. Yang, *Phys. Rev.* **150**, 327 (1966).
- [16] M. Gaudin, *Phys. Lett. A* **24**, 55 (1967).
- [17] H. Castella and X. Zotos, *Phys. Rev. B* **47**, 16186 (1993).
- [18] D. M. Gangardt and A. Kamenev, *Phys. Rev. Lett.* **102**, 070402 (2009).
- [19] M. Schechter, D. M. Gangardt, A. Kamenev, *Ann. Phys.* **327**, 639 (2011).
- [20] H. P. Büchler, V. B. Geshkenbein, and G. Blatter, *Phys. Rev. Lett.* **87**, 100403 (2001).
- [21] G. E. Astrakharchik and L. P. Pitaevskii, *Phys. Rev. A* **70**, 013608 (2004).
- [22] See Supplemental Material at [URL] for a detailed analysis within the Gross-Pitaevskii framework and a brief derivation of Eqs. (7), (9).
- [23] While the impurity gains the supercurrent momentum $n\Delta\Phi$, it loses a compensating amount of *core* momentum associated with the change in velocity.
- [24] A derivation of Eq. (6) can also be obtained from the effective field theory model of Refs. [11–13]. It consists of replacing $d^\dagger d \rightarrow \delta(x - X)$ with X the impurity coordinate, while also performing a canonical transformation to phononic fields in the presence of the equilibrated dressed impurity, namely $\rho = \tilde{\rho} - N\delta(x - X)$; $u = \tilde{u} - \frac{\Phi}{m}\delta(x - X)$. This transformation generates Eq. (6) with the understanding that Φ, N are related by a linear combination to the chiral phase shifts δ_\pm, β_\pm defined in Refs. [12, 13], Ref. [11], respectively.
- [25] V. N. Popov, *Functional Integrals and Collective Excitations* (Cambridge University Press, 1988).
- [26] F. D. M. Haldane, *Phys. Rev. Lett.* **47**, 1840 (1981).
- [27] M. Khodas, A. Kamenev, and L. I. Glazman, *Phys. Rev. A* **78**, 053630 (2008).
- [28] A. J. Leggett, S. Chakravarty, A. T. Dorsey, M. P. A. Fisher, A. Garg, and W. Zwerger, *Rev. Mod. Phys.* **59**, 1 (1987).
- [29] This may also be seen explicitly for a weakly coupled impurity using a Golden rule calculation with the dynamic structure factor of the liquid, similar to the calculation of the drag force in Ref. [21]. One then finds $M_c = mK$ and a lifetime $\tau_L \sim (c/V)^{2K-1}$.
- [30] A. O. Caldeira and A. J. Leggett, *Ann. Phys.* **149**, 374 (1983).
- [31] A. H. Castro Neto and M. P. A. Fisher, *Phys. Rev. B* **53**, 9713 (1996).
- [32] L. P. Pitaevskii and S. Stringari, *Bose-Einstein Condensation* (Clarendon Press, Oxford 2003).
- [33] T. Tsuzuki, *J. Low Temp. Phys.* **4**, 441 (1971).
- [34] V. Hakim, *Phys. Rev. E* **55**, 2835 (1997).
- [35] D. Taras-Semchuk and J. M. F. Gunn, *Phys. Rev. B* **60**, 13139 (1999).